X-ray observations of PKS 0745-191 at the virial radius: are we there yet?

D. Eckert[1], S. Molendi[1], F. Gastaldello[1,2], and M. Rossetti[1]

[1] INAF/IASF-Milano, via E. Bassini 15, 20133 Milano, Italy
    e-mail: eckert@iasf-milano.inaf.it
[2] University of California at Irvine, 4129, Frederick Reines Hall, Irvine, CA, 92697-4575, USA

ABSTRACT

Aims. We reassess the properties of the ICM at large radii in the galaxy cluster PKS 0745-191 in light of recent *Suzaku* measurements.
Methods. We analyze an archival 10.5 ks ROSAT/PSPC observation to extract the surface-brightness profile of PKS 0745-191 and infer the deprojected density profile. We then compare the ROSAT surface-brightness profile with the *Suzaku* result. We perform a mass analysis by combining the ROSAT density profile and the published temperature profiles from different instruments.
Results. We find that the ROSAT surface-brightness profile is statistically inconsistent (7.7σ) with the *Suzaku* result around and beyond the value of r_{200} estimated by *Suzaku*. We argue that, thanks to its large field of view and low background, ROSAT/PSPC is to the present day the most sensitive instrument for studying low surface-brightness X-ray emission in the $0.4-2.0$ keV band. We also note that the *Suzaku* temperature and mass profiles are at odds with the results from at least two other satellites (*XMM-Newton* and Swift).
Conclusions. The difference in surface brightness between ROSAT and *Suzaku* is most likely explained by the existence of additional foreground components at the low Galactic latitude of the source, which were not taken into account in the *Suzaku* background modeling. In light of our mass analysis, we conclude that any estimate of the fraction of the virial radius reached by X-ray measurements is affected by systematic errors of the order of 25%. As a result, the properties of the ICM at the virial radius are still uncertain, and the *Suzaku* results on PKS 0745-191 should be considered with caution.

Key words. galaxies: clusters: individual: PKS 0745-191 – X-rays: galaxies: clusters – galaxies: clusters: intracluster medium

1. Introduction

Observing the outskirts of galaxy clusters is important for understanding the formation processes of large-scale structures. For instance, studying the intracluster gas around the virial radius gives an opportunity to measure the transition between the gravitationally-bound gas of clusters and the infalling material from large-scale structures. Tracing the gas out to the virial radius is also important for calibrating the X-ray mass measurements, which are important to cosmology (e.g., Voit 2005). However, measuring the properties of the intracluster medium in cluster outskirts is difficult because of the low surface brightness of these regions. An instrument with a low internal background is required to measure the source emission at high radii. In the past few years, the *Suzaku* satellite achieved a breakthrough in this domain, performing measurements of the thermodynamical properties of the ICM out to the virial radius (Bautz et al. 2009; Reiprich et al. 2009; Hoshino et al. 2010; Kawaharada et al. 2010).

PKS 0745-191 ($z = 0.1028$) is a very luminous ($L_X \sim 3 \times 10^{45}$ erg s^{-1} in the $2-10$ keV band, Arnaud et al. 1987; Allen et al. 1996), cool-core cluster located in the vicinity of the Galactic plane ($b = +3°$). From a *Suzaku*/XIS observation of the cluster, George et al. (2009, hereafter, G09) measured the cluster emission out to $\sim 1.5\ r_{200}$, and determined a value of $r_{200} = 1.7$ Mpc (15.2 arcmin) for the virial radius. Surprisingly, the authors noted a flattening of the density and entropy profiles around r_{200}, at variance with results from cosmological simulations (e.g., Roncarelli et al. 2006; Tozzi & Norman 2001). This

and similar results from other authors inspired a large amount of theoretical work (e.g., Lapi et al. 2010; Nagai & Lau 2011), invoking several mechanisms (e.g., non-thermal pressure support, gas clumping) to reconcile simulations and observations. An independent confirmation of this result would therefore be very important to our understanding of cluster outskirts.

In this paper, we present the analysis of an archival ROSAT Position Sensitive Proportional Counter (PSPC) observation of PKS 0745-191, with the aim of confirming the result of G09. Although the PSPC could not measure temperatures because of its limited bandpass ($0.1-2.4$ keV), its low instrumental background and large field of view (~ 2 square degrees) made it an excellent tool for the study of low surface-brightness regions such as the outer regions of galaxy clusters (see e.g., Vikhlinin et al. 1999; Neumann 2005). We also perform a mass analysis using the PSPC density profile and the temperature measurements from various other X-ray satellites, and compare the results with the measurements of G09. The paper is organized as follows. In Sect. 2, we describe the data analysis procedure. We present our results for the density profile of the cluster in Sect. 3, and discuss them in Sect. 4.

Throughout the paper, we assume a ΛCDM cosmology with $\Omega_m = 0.3$, $\Omega_\Lambda = 0.7$, and $H_0 = 70$ km s^{-1} Mpc^{-1}.

2. Data analysis

2.1. Reduction

PKS 0745-191 was the target of a pointed ROSAT/PSPC observation on October 15, 1993 (observation ID RP800623N00)
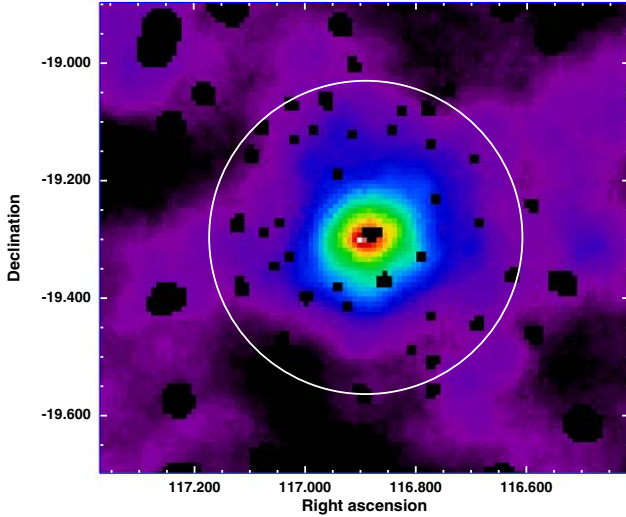
Fig. 1. Background-subtracted (NXB+SSX), exposure-corrected, adaptively smoothed ROSAT/PSPC image of PKS 0745-191. The black areas indicate the position of masked point sources. The white circle shows the approximate location of r_{200} as estimated by G09.

Fig. 2. Fit of the SB profile in the 25-50 arcmin radial range by a constant to estimate the cosmic background component (blue). For comparison, the NXB+SSX profile is shown in red. The bottom panel shows the deviations of the data points to the model in units of σ.

for a total of 10.5 ksec. We reduced the data using the ROSAT Extended Source Analysis Software (ESAS, Snowden et al. 1994). To eliminate flaring periods, we extracted a light curve from the raw event files and rejected all time periods where the Master Veto count rate was above 220 counts s^{-1}. We then used the ESAS task *ao* to create a model of the scattered solar X-ray background (SSX, Snowden & Freyberg 1993), and generated a particle background model using the *cast_part* executable (Snowden et al. 1992; Plucinsky et al. 1993). The total model for the non X-ray background (NXB) and the SSX was then inferred.

A counts image in the 0.4−2.0 keV band was then extracted from the cleaned event file and the corresponding exposure map was created using the task *cast_exp*. Point sources were then detected from the image (using the program *detect*) and a point source mask was generated to excise the corresponding regions. As a result, a background-subtracted, exposure-corrected image was created and adaptively smoothed. In Fig. 1, we show the resulting image together with the position of r_{200} estimated by G09. Point sources have been masked from the image.

2.2. Density profile

To measure the density profile of the cluster, we first extracted the surface-brightness (SB) profile of the source following the procedure described in Eckert et al. (2011). We used the total counts image and the exposure map to extract the mean count rate in concentric annuli out to a radius of 50 arcmin with a bin size of 1 arcmin. The NXB and SSX profiles were also extracted using the same procedure from the background image and subtracted from the total profile.

To subtract the cosmic background component, we fitted the SB profile in the 25−50 arcmin radial range ($r > 1.6 r_{200}$) with a constant (see Fig. 2). The bins were grouped to ensure a minimum number of 200 counts per bin. The profile in this radial range is accurately-described by a constant ($\chi^2 = 18.6/21$ d.o.f.). We verified that the background determination does not change significantly when using a different radial range by repeating the same procedure in the radial ranges 25−45,
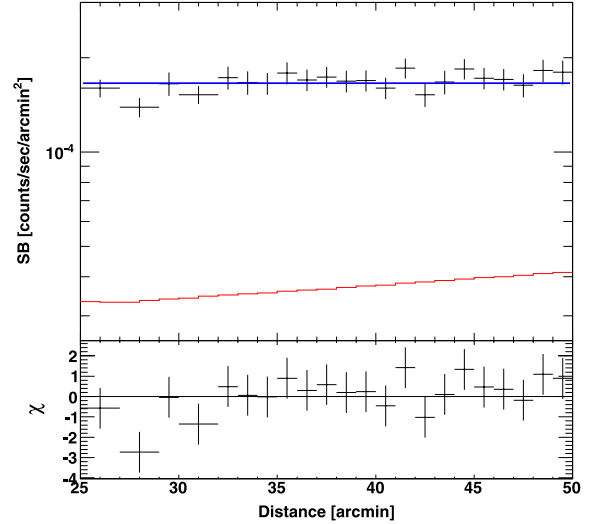
30−45, 25−40, 30−50, and 35−50 arcmin. In all cases, we find that the measured background value is consistent to within 1σ with the value extracted from the total 25−50 arcmin range, which indicates that our background determination is stable. The resulting background value was then subtracted from the total profile, and the uncertainties in the background determination were propagated to the background-subtracted profile. In Fig. 2, we show the surface-brightness profile in the 25−50 arcmin range together with the best-fit value for the sky background (blue) and the NXB+SSX profile (red). We can see that at all radii the cosmic component is dominant relative to the NXB and the SSX.

From the background-subtracted profile, we used the procedure of Kriss et al. (1983) to deproject the surface-brightness profile. We assumed the temperature profile of G09, and used XSPEC v12.6.0 and the PSPC effective area to convert the PSPC count rate per unit volume into emissivity using the normalization of the MEKAL model

$$\text{Norm} = \frac{10^{-14}}{4\pi[d_A(1+z)]^2} \int n_e n_H \, dV, \tag{1}$$

where $n_e \sim 1.2 n_H$. We note that in the 0.4−2.0 keV band the conversion factor is insensitive to temperature. For temperatures between 2 and 8 keV, the conversion from PSPC count rate to emissivity changes by at most 4%. Assuming spherical symmetry and a constant density within each shell, we deduced the density profile.

2.3. Error estimate

A crucial point for our analysis is the estimate of statistical uncertainties in the density profile. To compute the error bars in the density profile, we used a Monte Carlo approach to analyzing the ROSAT image. Assuming Poisson statistics, we generated 10^8 realizations of the PSPC counts profile, and performed the procedure described above to obtain 10^8 realizations of the density profile. The error bars and confidence intervals were then calculated from the distribution of values in each density bin. When a negative background-subtracted profile was found, the density was set to 0. We then defined a 90% upper limit by the
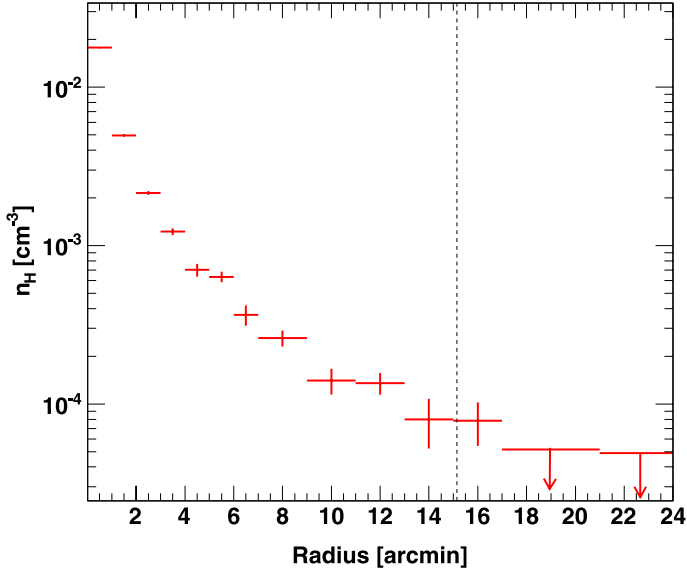
Fig. 3. ROSAT/PSPC density profile. The error bars and upper limits were estimated from Monte Carlo simulations (see text). The dotted black line shows the approximate location of r_{200} computed by G09.

Fig. 4. Background-subtracted (cosmic+NXB) ROSAT/PSPC surface-brightness profile (red), compared to the *Suzaku* profile from G09 folded through the PSPC response (black).

value for which 90% of the simulations give a result below this value.

3. Results

In Fig. 3, we show the resulting ROSAT/PSPC density profile. The dotted black line shows the estimate of r_{200} from G09. Beyond $r = 17'$, we do not detect any significant cluster emission, and set an upper limit to the density in the $17-25'$ range of $n_{17-25'} < 4.2 \times 10^{-5}$ cm^{-3} (90% confidence level).

To compare the ROSAT and *Suzaku* profiles, we used a method similar to the one reported in Bowyer & Vikhlinin (2004). More specifically, we converted the projected *Suzaku* profile into the MEKAL normalization (Eq. (1)), and folded it through the response of ROSAT/PSPC to compute the count rate that should be seen by PSPC. The resulting profile (black), compared to the background-subtracted PSPC profile with the same binning (red), is shown in Fig. 4. While in the inner 4 annuli the profiles differ by only ∼11% (the difference in the innermost 2 bins being explained by the broader *Suzaku* PSF), a clear discrepancy between the ROSAT and *Suzaku* profiles is found beyond 13.5′. In the 13.5−18.5 arcmin bin, the *Suzaku* profile exceeds the ROSAT data point by a factor of three, while in the 18.5−24 arcmin bin our 90% upper limit lies a factor of 2.1 below the *Suzaku* detection. The profiles at the largest radii are discrepant at more than 7.7σ. This result is stable in terms of background level. We indeed reach the same conclusion when we use the lowest allowed value for the background instead of the mean value.

4. Discussion

As shown above, our ROSAT/PSPC density profile is statistically inconsistent with the *Suzaku* profile from G09 at high significance. We discuss here several possibilities to reconcile the two results.

1. *Cross-calibration*: as found in the case of ROSAT/PSPC and *XMM-Newton*/MOS2 (see Appendix A of Eckert et al. 2011),
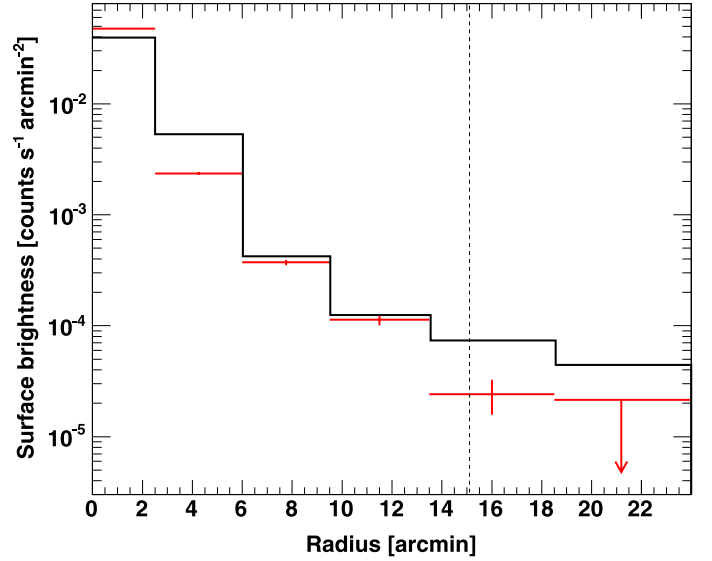
there could be a cross-calibration discrepancy between PSPC and *Suzaku*/XIS. However, as shown in Fig. 4 below 13.5 arcmin the projected profiles agree to within 11%, while at the largest radii the ROSAT data points are below the *Suzaku* measurements by a factor of 2.1−3.0. Thus, although a cross-calibration problem may exist, it certainly cannot explain the observed discrepancy.

2. *Absorption*: because of its softer bandpass, ROSAT is more affected than *Suzaku* by absorption, which is large at the position of PKS 0745-191 ($N_H = 4.2 \times 10^{21}$ cm^{-2}). If the Galactic absorption is significantly larger in the outskirts of the cluster ($N_H \gtrsim 10^{22}$ cm^{-2}) than in the center, the flux observed in the *Suzaku* data can be suppressed in the ROSAT band. Variations in the N_H on these scales (∼200 arcmin^2) should produce significant variations (by a factor of ∼2.2) in the CXB intensity in the ROSAT band. However, an analysis of the background beyond 25 arcmin from the cluster center did not show any significant variations in the background level. It therefore seems very unlikely that these variations are present only along the line of sight of the cluster.

3. *Spatial coverage*: because of the smaller field of view (FOV) of *Suzaku*, the G09 result was extracted in a rather small region (see Fig. 1 of G09). If the gas density varied significantly at large radii (as in the case of A1795, Bautz et al. 2009), the regions selected in the *Suzaku* observation might have a higher density, hence would not be representative of the mean density around the virial radius. However, extracting the surface-brightness profile in exactly the same region as G09, we do not find any significant difference from the mean profile. In this specific region, the discrepancy with *Suzaku* is still statistically significant (5.2σ in the last two bins).

4. *Background determination*: because of the very low surface brightness of the cluster emission around r_{200}, the background determination is important when measuring the physical properties of the gas in these regions. Thanks to its much wider FOV, ROSAT has a clear advantage with respect to *Suzaku*. The large ROSAT FOV allows us to perform a local background measurement, while G09 had to rely on background modeling. At the low Galactic latitudes where PKS 0745-191 is located, the foreground emission associated

with our galaxy is known to be stronger and more variable than at higher latitudes, making background characterization a more complicated business. Thanks to its higher spatial resolution and larger FOV, ROSAT is able to more accurately measure the total sky background emission, and resolve a larger fraction of sources (see Fig. 1), so the systematic uncertainties affecting the ROSAT measurements are smaller than those of *Suzaku*.

An additional background component is probably causing the discrepancy. G09 used an earlier observation of the Lockman hole to estimate the cosmic background component, arguing that, since the total cosmic background level measured by ROSAT in the $1-2$ keV band at the position of PKS 0745-191 is similar to the one for the Lockman hole, the same model could be used for the sky background in the two observations. However, since the extragalactic background at the low Galactic latitude of PKS 0745-191 is lower because of the larger absorption, another component, most likely Galactic, must be responsible for compensating the decrease in the extragalactic emission. Masui et al. (2009) presented the *Suzaku* spectrum of an empty field located only 3° away from PKS 0745-191. The authors found clear evidence of another sky component at a temperature of ~0.8 keV, with excess emission in the $1-1.2$ keV range suggesting that even higher temperature emission exists. This implies that the spectrum is qualitatively unlike empty-field spectra extracted at high Galactic latitude. Since G09 neglected these components, their results are likely to be affected by an incorrect background model, implying that clusters located at low Galactic latitude (or in any region with complicated soft emission, such as the North polar spur) are not ideal targets for the study of cluster outskirts.

In low-SB regions, the key feature for an instrument is the ratio of background level to effective area (Ettori & Molendi 2011). In this respect, ROSAT/PSPC is a more sensitive instrument than *Suzaku*/XIS. From the total background level (see Fig. 2) we get a value of 4×10^{-7} counts s^{-1} keV^{-1} arcmin^{-2} cm^{-2} for this quantity ($0.4-2.0$ keV band), which is almost a factor of two lower than for *Suzaku*/XIS (see Fig. 5 of Mitsuda et al. 2007).

As stated in G09, the mass parameters derived from the *Suzaku* data appear to be inconsistent with other results. We performed a mass analysis using the ROSAT density profile and the temperature profiles from various satellites (*Suzaku*, *XMM*, *BeppoSAX* and Swift, see Appendix A). Interestingly, we see that all satellites except *Suzaku* find a value of r_{200} that is larger than 2 Mpc (~25% larger than the value estimated by G09), corresponding to a difference of a factor of 2 in the virial mass. For *XMM* and Swift measurements the difference in r_{200} is statistically highly significant, at more than 6 and 5σ, respectively (see Appendix A for details).

Since there is no compelling reason to prefer one set of measurements with respect to another, we are forced to conclude that the scale radius in PKS 0745-191 is currently affected by a systematic indetermination of roughly 25%. It goes almost without saying that any estimate of the fraction of the virial radius reached by X-ray measurements will have to take this indetermination into account. This is no small issue. Depending on whether we assume the *Suzaku* or the *XMM*/Swift virial radius we have that the PSPC surface brightness measurements extend to 1.03 r_{200} or 0.8 r_{200}. Finally, although we cannot prefer one estimate of r_{200} to another, there are arguments favoring the *XMM*/Swift measurement over the *Suzaku* one. First of all, we have two independent measurements that are consistent with

one another and inconsistent with the *Suzaku* one. Secondly, the Swift and *XMM* profiles are consistent with mean cluster temperature profiles measured with *BeppoSAX* (De Grandi & Molendi 2002), *XMM* (Leccardi & Molendi 2008), and *Chandra* (Vikhlinin et al. 2006), and with predictions from simulations (e.g., Roncarelli et al. 2006). This is not the case for the *Suzaku* profile, which shows a much more rapid and significant decline. This is an important point since, as discussed in the Appendix, the difference in r_{200} follows from the difference in the shape of the radial temperature profiles.

5. Conclusion

We have reported our analysis of an archival ROSAT/PSPC observation of the galaxy cluster PKS 0745-191. We have found that the surface-brightness profile extracted from PSPC data is statistically inconsistent with the *Suzaku* result from G09 at high significance (7.7σ). At large radii (>13.5 arcmin), the predicted count rate exceeds the PSPC data by a factor of $2.1-3$. This difference is most likely due to a problem in the modeling of the background in the *Suzaku* measurement, which is difficult for a narrow-field instrument at the low Galactic latitude of the source. Thanks to its larger FOV and higher spatial resolution, ROSAT is able to measure the background more accurately than *Suzaku*.

We have also shown that the rapidly declining temperature profile measured by *Suzaku* leads to total mass and r_{200} estimates at variance with those derived from Swift and *XMM* temperature profiles. In the absence of compelling proof favoring one measurement over another, we conservatively conclude that any estimate of the fraction of the virial radius reached by X-ray measures is affected by a systematic error of about 25% associated with the indetermination in r_{200}. In conclusion, we stress that the current observational knowledge of the ICM properties of PKS 0745-191 at large radii is still uncertain, thus the results presented by G09 should be considered with care.

Appendix A: Mass analysis with different datasets

We performed a mass analysis adopting method 2 of Ettori et al. (2010, and references therein) using the ROSAT surface brightness profile (this work). For the temperature profile, we adopted the published temperature profiles of four different instruments: *XMM-Newton* (Snowden et al. 2008), *BeppoSAX* (De Grandi & Molendi 2002), Swift/XRT (Moretti et al. 2011), and the *Chandra* and *Suzaku* temperature profile of G09 (their Fig. 5, i.e. excluding the Chandra data points within 70 kpc and the innermost and outermost Suzaku data points). In Fig. A.1, we plot the temperature profiles for PKS 0745-191 within the inner 15 arcmin from the center of the cluster, obtained by various satellites with very different instruments (gas proportional counters or CCDs) in very different orbits (low Earth orbits (LEO) with very low particle background such as *BeppoSAX* and Swift/XRT, or highly elliptical orbits with high background such as XMM). There is a clear discrepancy between the behavior of the *Suzaku* profile compared to all the other satellites.

In Table A.1, we give the best-fit parameters for the NFW profile estimated using the different datasets. We can see that

Table A.1. Best-fit parameters of the NFW profile to the ROSAT density and several published temperature profiles (see Fig. A.1).

	ROSAT+*XMM*	ROSAT+*Suzaku*	ROSAT+*SAX*	ROSAT+Swift
c_{200}	3.45 ± 0.25	9.05 ± 0.16	4.89 ± 0.89	3.52 ± 0.26
r_s	697 ± 77	207 ± 2	434 ± 137	689 ± 76
r_{200}	2405 ± 82	1878 ± 33	2124 ± 160	2429 ± 92
M_{200}	17.48 ± 1.85	8.32 ± 0.41	12.03 ± 3.04	18.00 ± 2.05
χ^2/d.o.f.	$57/23$	$42/20$	$27/18$	$61/19$
r_{xsp}	1587	2097	1360	1247

Notes. The parameters are the concentration (c_{200}), NFW scale radius (r_s) in kpc, r_{200} in kpc, and gravitational mass (M_{200}) in units of 10^{14} $M_\odot$. The last parameter, r_{xsp}, denotes the maximum radius at which temperature measurements could be performed, in kpc.
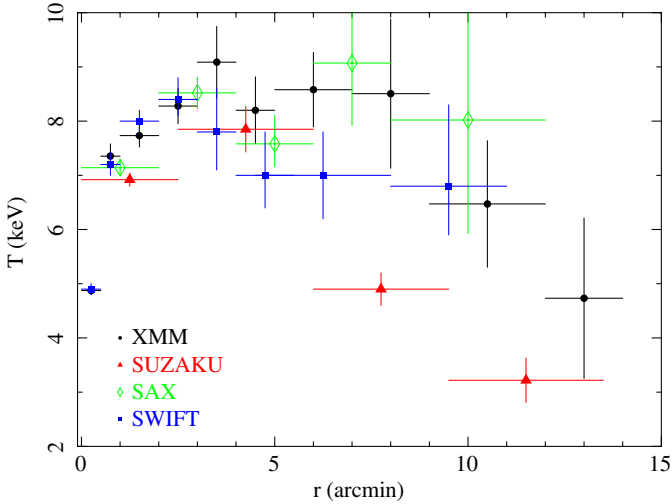

Fig. A.1. Temperature profiles of PKS 0745-191 measured by *Suzaku* (red triangles, G09), *XMM-Newton* (black circles, Snowden et al. 2008), Swift/XRT (blue squares, Moretti et al. 2011) and *BeppoSAX* (green diamonds, De Grandi & Molendi 2002).

XMM-Newton, *BeppoSAX*, and Swift data give results in good agreement, and point towards a value of r_{200} larger than 2 Mpc. In contrast, if we use the *Chandra* and *Suzaku* profile of G09 we obtain results in agreement with theirs, $r_{200} = 1.88 \pm 0.03$ Mpc and $M_{200} = (8.32 \pm 0.41) \times 10^{14}$ $M_\odot$, notwithstanding the different methods adopted in the mass analysis, for example the use of the ROSAT density profile and the simplifying assumptions of constant density within each shell and estimate of the volume defined by G09. G09 correctly points out the problems of the NFW fits applied to the *Chandra* data because the data do not extend to the NFW scale radius, r_s. The mass fits reported in Table A.1 all use the ROSAT surface brightness profile extending to 1927 kpc and the spectroscopic temperature data out to the radius listed as r_{xsp} for the various satellites. A necessary ingredient for a reliable measurement of the NFW parameters is that the fitted value of r_s lies well within the outer radius of the X-ray data, which is fulfilled by all the adopted datasets. Between *XMM-Newton* and *Suzaku*, the discrepancy is at the 6σ and 4.8σ level for r_{200} and M_{200}, respectively. The results are at odds at the level of 5.6σ and 4.6σ between Swift and *Suzaku*, and 1.5σ and 1.2σ between *BeppoSAX* and *Suzaku*.

These results clearly highlight the importance of the *Suzaku* temperature profile for the rather low values of r_{200} and M_{200} obtained in G09 compared to those obtained from *XMM-Newton*, *BeppoSAX*, and Swift data sets. The discrepancy can be quantified by comparing the value for the slope of the power-law fit to the temperature profile excluding the core as reported by G09, -0.94 ± 0.06, to the mean values of observed temperature profiles beyond 0.2 r_{180} as reported by Leccardi & Molendi (2008), -0.31 ± 0.02, i.e. a 10σ deviation from the mean. The inconsistency with the milder decline found in hydrodynamical simulations (e.g., Roncarelli et al. 2006) was also noted by G09.

References

Allen, S. W., Fabian, A. C., & Kneib, J. P. 1996, MNRAS, 279, 615
Arnaud, K. A., Johnstone, R. M., Fabian, A. C., et al. 1987, MNRAS, 227, 241
Bautz, M. W., Miller, E. D., Sanders, J. S., et al. 2009, PASJ, 61, 1117
Bowyer, S., & Vikhlinin, A. 2004, J. Korean Astron. Soc., 37, 579
De Grandi, S., & Molendi, S. 2002, ApJ, 567, 163
Eckert, D., Molendi, S., & Paltani, S. 2011, A&A, 526, A79
Ettori, S., & Molendi, S. 2011, Mem. Soc. Astron. Ital. Supp., 17, 47
Ettori, S., Gastaldello, F., Leccardi, A., et al. 2010, A&A, 524, A68
George, M. R., Fabian, A. C., Sanders, J. S., Young, A. J., & Russell, H. R. 2009, MNRAS, 395, 657
Hoshino, A., Patrick Henry, J., Sato, K., et al. 2010, PASJ, 62, 371
Kawaharada, M., Okabe, N., Umetsu, K., et al. 2010, ApJ, 714, 423
Kriss, G. A., Cioffi, D. F., & Canizares, C. R. 1983, ApJ, 272, 439
Lapi, A., Fusco-Femiano, R., & Cavaliere, A. 2010, A&A, 516, A34
Leccardi, A., & Molendi, S. 2008, A&A, 486, 359
Masui, K., Mitsuda, K., Yamasaki, N. Y., et al. 2009, PASJ, 61, 115
Mitsuda, K., Bautz, M., Inoue, H., et al. 2007, PASJ, 59, 1
Moretti, A., Gastaldello, F., Ettori, S., & Molendi, S. 2011, A&A, 528, A102
Nagai, D., & Lau, E. 2011, ApJ, 731, L10
Neumann, D. M. 2005, A&A, 439, 465
Plucinsky, P. P., Snowden, S. L., Briel, U. G., Hasinger, G., & Pfeffermann, E. 1993, ApJ, 418, 519
Reiprich, T. H., Hudson, D. S., Zhang, Y., et al. 2009, A&A, 501, 899
Roncarelli, M., Ettori, S., Dolag, K., et al. 2006, MNRAS, 373, 1339
Snowden, S. L., & Freyberg, M. J. 1993, ApJ, 404, 403
Snowden, S. L., Plucinsky, P. P., Briel, U., Hasinger, G., & Pfeffermann, E. 1992, ApJ, 393, 819
Snowden, S. L., McCammon, D., Burrows, D. N., & Mendenhall, J. A. 1994, ApJ, 424, 714
Snowden, S. L., Mushotzky, R. F., Kuntz, K. D., & Davis, D. S. 2008, A&A, 478, 615
Tozzi, P., & Norman, C. 2001, ApJ, 546, 63
Vikhlinin, A., Forman, W., & Jones, C. 1999, ApJ, 525, 47
Vikhlinin, A., Kravtsov, A., Forman, W., et al. 2006, ApJ, 640, 691
Voit, G. M. 2005, Rev. Mod. Phys., 77, 207